Effect of behavioral parameters of base isolators on the seismic response of the bridge to near-fault ground motions

Abbas Keramati, Gholamreza Nouri*

Faculty of Engineering, Kharazmi University, Tehran, Iran

ABSTRACT: The current study examined the effectiveness of considering the nonlinear behavior of lead rubber bearings (LRBs) on the response of seismically isolated bridges. Also, the effect of the vertical component of the strong ground motion on the critical buckling capacity of LRBs was studied. 3D modeling of a seismically isolated bridge with nonlinear time history analysis under near-fault ground motion was applied. The results showed lack of consideration of the cavitation, post-cavitation and strength degradation behavior in tension and force softening under compression produces a large axial force and small axial displacement in LRBs and axial force-deformation appears to be perfectly linear. The results revealed that the average maximum base shear force in the bridge piers increased by 116% and 29.8% in the longitudinal and transverse direction respectively in comparison with the simple modeling. It also increased the average maximum displacement of bridge pier about 113% in the longitudinal direction and 31% in the transverse direction. Simplifying the LRBs modeling led to produces smaller stress and base shear forces of the bridge columns relative to actual conditions. Since the AASHTO regulation requires a seismically isolated bridge substructure to remain in the linear range, so in the bridges with a simplified model of LRBs, the nonlinear behavior of some columns of isolated bridges will be ignored under strong near-fault ground motion.

1. INTRODUCTION

The behavior of an elastomeric bearing such as lead rubber bearings (LRBs) is highly nonlinear and more complicated than other structural components under strong ground motion and is a function of their inherent properties that can be influenced by several factors. Thus, dynamic responses to earthquake excitation that ignore these properties can result in unrealistic responses. Saiidi *et al.* (1999) studied the nonlinear seismic behavior of multi-column bridges with base isolation. They revealed that the use of base isolators does not necessarily increase superstructure displacement during earthquakes. Moreover, the proper design of isolators can decrease the ductility demand on reinforced concrete bridges [1]. The behavioral properties of elastomeric bearings under strong ground excitation will vary over time. This creates challenges for those who are trying to model elastomeric bearing responses. The objectives for elastomeric bearings that are the main aspects of modeling were introduced [2] as being:

· Coupling of bi-directional motion in the horizontal directions;
· Coupled vertical and horizontal motion;
· Cavitation and post-cavitation in tension;
· Strength degradation in cyclic tensile loading due to cavitation;

*Corresponding author's email: r.nouri@khu.ac.ir

· Strength degradation in cyclic shear loading due to heating of the lead core and;
· Variation in critical buckling load capacity due to lateral displacement

The fundamental period of an isolated structure increases as the flexibility of the elastomeric bearings increases that reduce seismic forces in the superstructure. However, this reduction could lead to large horizontal displacement in the isolators along with lateral flexibility that could seriously decrease the critical axial load capacity of an isolator. The experimental results were indicated that the critical load and the horizontal stiffness decreases as horizontal displacement and axial loading increase.[3, 4]. Kumar et al. (2015) characterized the behavior of elastomeric bearings in tension by experimental investigation. The effect of cavitation on the shear and axial properties of elastomeric bearings was investigated by performing post-cavitation tests. The result of experimental tests showed that the pre-cavitation tensile stiffness decreases with an increase in coexisting shear strain [5]. The mechanical model for predicting the behavior of elastomeric seismic isolation bearings subjected to combined end rotations and shear deformation was studied by Ishii et al. (2017). The test results indicated that bearing rotational stiffness increases with increasing vertical load but decreases with the increasing shear deformation [6]. Ishii & Kikuchi (2019) improved numerical analysis for the ultimate behavior

of elastomeric seismic isolation bearings [7]. Result of the study on the critical behavior of isolator under tension–shear load showed that the critical load decreases nonlinearly with the increase of horizontal shear strain, which reveals that it is unreasonable to define the threshold value of tension independent of the amount of horizontal shear strain [8].

Nonlinear rotational constitutive law for predicting critical loads in elastomeric isolation bearings was improved by Zhang et al. (2016). The improved model can provide a continuous prediction of critical loads throughout the horizontal displacements [9].

Recent research and earthquake experience have shown that the inclusion of the vertical components of ground motion in the analysis and the design of structures is essential [10]. For near-fault earthquakes, the vertical component may significantly exceed the horizontal spectra for short periods [11]. Eröz and DesRoches (2013) found that excluding the vertical component of the ground motion in the analysis of lead rubber (LR) isolators may overlook a fundamental failure mode [12]. Warn and Whittaker (2008) examined LR base isolators under earthquake simulation testing. Their results showed that the vertical component of excitation significantly amplified (2 to 5.5 times) the vertical response of the elastomeric isolator. The study also demonstrated that the sum of the maximum values through the vertical component of the ground motion and the overturning moment is a conservative approach, as those values are unlikely to occur coincide [13]. Button *et al.* (2002) investigated the effect of vertical ground motion on the seismic response of a variety of highway bridges. The results illustrated that the vertical component of excitation could have a significant effect on the axial load on the pier and shear forces on the vertical deck [14].

Chen *et al.* (2014) suggested a theoretical model to analyze rubber bearings based on the theory of elasticity. By applying boundary conditions and assuming incompressibility, they formulated stress-deformation expressions for tensile rubber [15]. The effects of the nonlinear behavior of isolation pads on the seismic response of isolated bridges were studied by Olmos and Roesset (2010). Their results showed the importance of considering the nonlinear behavior of pads on the seismic

response of the isolated bridges [16].

The present study models two seismically isolated bridges. The first is designed by modeling of LRBs by considering the fundamental features for nonlinear behavior of isolators introduced by Kumar *et al.* (2014) [2] . The second uses a common simplified model for load-deformation of the isolator. Nonlinear time history analysis is performed in OpenSees software under near-fault strong ground motion. The responses of the different isolated bridges are compared to show the importance of considering the main behavioral specifications of LRs on the seismic response of bridges. The effect of the vertical component of the strong ground motion on the critical buckling capacity of LRBs is studied for a typical highway bridge.

2. BRIDGE MODEL

The Kurdistan Highway Bridge located in Tehran was selected for modeling. The bridge is located in the vicinity of major north-east faults in Tehran.

2.1 Bridge substructure

The modeled bridge has a symmetrical two-way form (Fig.1) and there was no connection or constraint between the two ways. The total length of the bridge with ramps is 485.6 m. The bridge length is 229 m and has 8 spans. The length of the first and last spans is 24.5 m and the middle spans are 30.0 m. This overpass bridge has seven reinforced concrete piers, each pier having two circular columns 1.2 m in diameter with a 7.5-cm cover thickness (Fig.2).

2.2 Bridge superstructure

The bridge deck was formed of six continuous steel girders and a 20-cm-thick concrete slab (Fig.1). The weight of superstructure was 51000 kN for two ways. The bridge live load was under AASHTO criteria at 12000 kN. Because the bridge is an urban one, 50% of the bridge live load was considered when modeling to apply time history analysis.

2.3 Bridge modeling

Seismic isolation of the bridge was achieved by placing isolators under each of the girders above the piers and
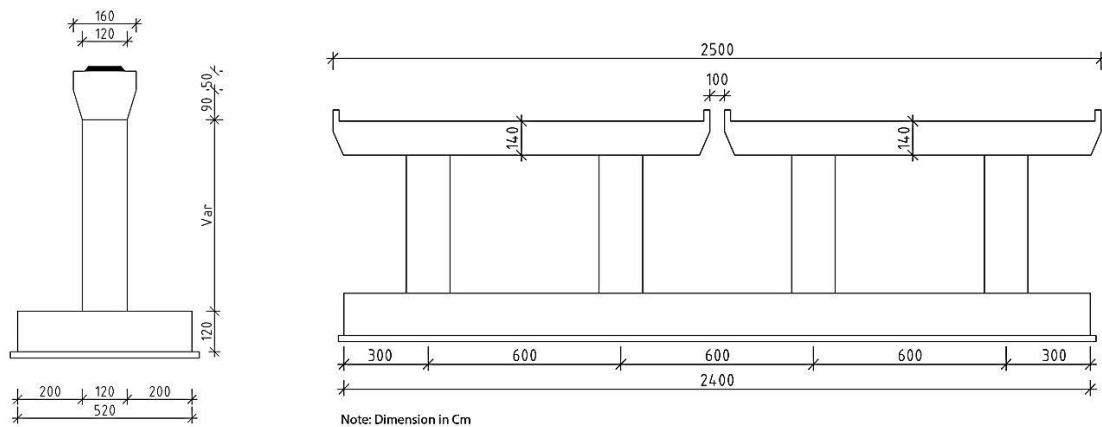
Fig.1. Bridge cross section and Pier details
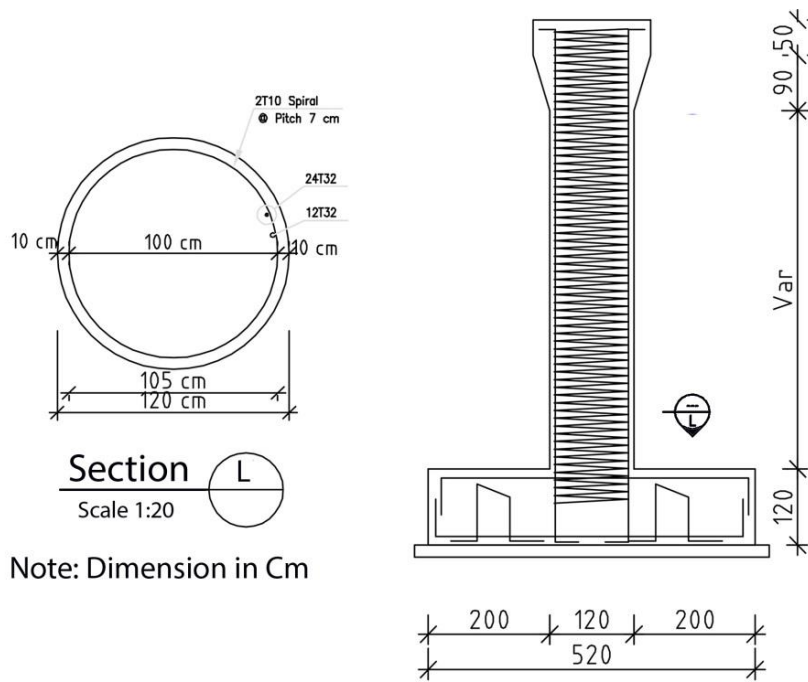
Fig. 2. Bridge circular column cross sections and reinforcing detail
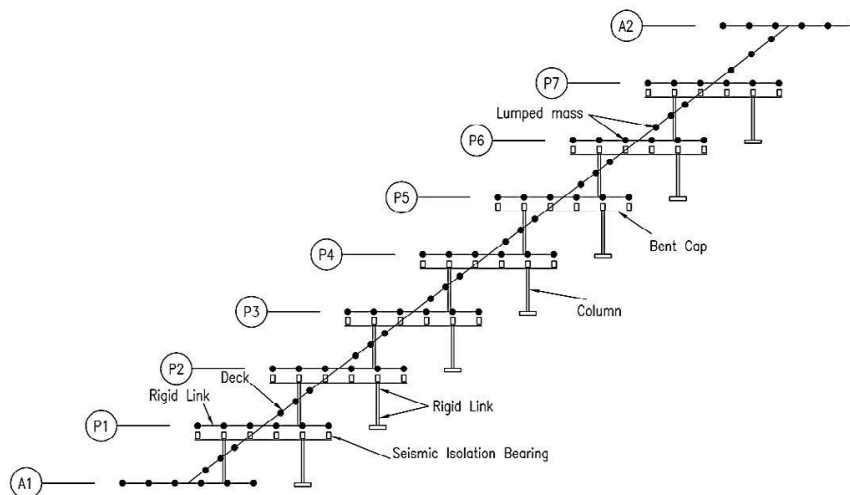
Fig. 3. Model of seismically isolated bridge in OpenSees

abutments. A 3D finite element model of the bridge was developed in OpenSees (Fig.3).

The degrees of freedom and coordinate systems used to model the bridge in accordance with the coordinate system were proposed by Aviram *et al.* (2008) [17].

Abutments were modeled as simple supports. Nonlinear beam-column elements with fiber sections were used to model the columns and bent caps of the bridge piers. In the fiber sections, the uniaxial concrete material (Concrete03) object and the compressive strength, tensile strength and nonlinear tension softening of confined concrete were used to model the confined concrete. The uniaxial Kent-Scott-Park concrete material (Concrete01) object with degraded linear unloading/ reloading stiffness and no tensile strength was used to model

the unconfined concrete [18]. The compressive strength of confined and unconfined concrete were assumed to be 30 and 24 MPa, respectively. Uniaxial steel material (Steel01) with a yield stress of 300 MPa was used to model the behavior of the reinforcement steel. The bridge deck was modeled using the elastic beam-column element in the longitudinal direction. Table 1 shows the properties of two types of cross-section used in the deck element of bridge.

3. LEAD RUBBER BEARING SEISMIC ISOLATION

The LR seismic isolation system is elastomeric bearing. The seismic energy is dissipated by a lead core is inserted at the vertical centerline. The elastomeric bearings consist of several layers of rubber separated by thin steel shims. The rubber

Table 1. Properties of two different types of cross-section of bridge deck

Properties	Section properties located in the mid-span	Section properties located on the Pier
Cross section (m²)	4.2125	4.9714
Moment of inertia about y (I_{yy} m⁴)	55.4361	65.7016
Moment of inertia about z (I_{zz} m⁴)	1.622	1.8303
Torsional moment (J m⁴)	0.0347	0.0385
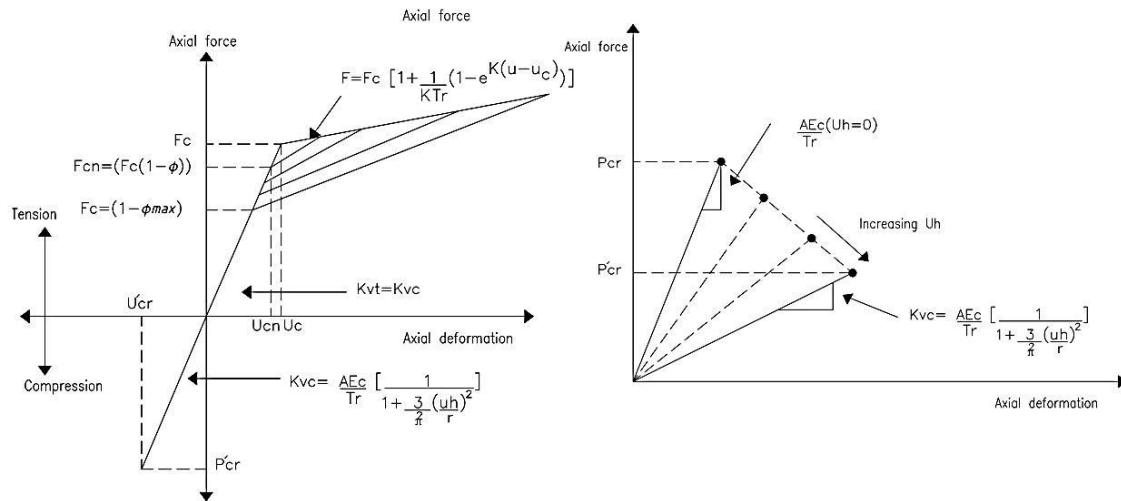
Fig. 4. Mathematical model of elastomeric bearings behavior in axial direction [2]

layers provide lateral flexibility while the steel shims increase the vertical stiffness to support large axial loads and prevent bulging of the rubber [19]. When the bearing and lead core deform under shear, the elastic stiffness of the lead provides the initial stiffness (K_u). Under increased lateral loading, the lead yields in a nearly perfectly plastic manner and the post-yield stiffness (K_d) is provided by the rubber alone [20, 21].

3.1 Design of LRB seismic isolation

In this paper, the LRB was designed in accordance with AASHTO specifications for seismic isolation design (2010) [22] using the direct displacement design method introduced by Buckle *et al.* (2011) [20]. The geometrical characteristics were obtained for the LR isolator based on their position on the bridge abutment (type 1), the last pier (type 2) or the middle pier (type 3).

Table 2 presents the results from the design of the LR isolator of the bridge.

3.2 Modeling of LR seismic isolation
3.2.1 Behavior under axial loading

A mathematical model proposed by Kumar *et al.* (2014) [2] has been applied to consider the main aspects of modeling. This model has been verified and validated by ASME (2006) [23] and was carried out in OpenSees software. The ElastomericX element was used to model the LR isolators to assign the yield force of the lead core. Fig.4 shows the mathematical model of an elastomeric bearing in the axial direction. The model

of Kumar *et al.* (2014) [2] uses three unknown parameters: cavitation k, strength degradation α and damage index $\varnothing_{max}$. Warn (2006) [24] and Kumar *et al.* (2014) proposed values of $k = 20$, $\varnothing_{max} = 0.75$ and $\alpha = 10$.

3.2.2 Horizontal stiffness of elastomeric bearing

While the axial load tends toward the critical buckling load capacity, the impact of axial load on the horizontal stiffness of an elastomeric bearing can be significant. Koh and Kelly (1987) [4] developed an equation for horizontal stiffness that depends on the axial load. An estimation of the expression for the horizontal stiffness that gives exceptionally precise results is given as Eq. (1) [2, 25].

$$K_H = \frac{GA}{T_r}\left[1-\left(\frac{P}{P_{cr}}\right)^2\right] = K_{H\blacklozenge}\left[1-\left(\frac{P}{P_{cr}'}\right)^2\right] \tag{1}$$

where $K_{H_{\circ}}$ is the horizontal stiffness at zero axial load, P_{cr}' is the instantaneous value of the critical buckling load, P is the instantaneous value of the axial load applied to the bearing, G is the shear modulus, A is the true area of the bearing and T_r is the total rubber thickness. The axial load-deformation curve in compression is shown in Fig. 4(b). In the figure, E_c is the compression modulus of the bearing calculated as the average axial stress divided by the average axial strain in a rubber layer and r is the radius of gyration of the bonded rubber area.

Table 2. Specification of designed LRB

Title	Type 1	Type 2	Type 3
Seismically isolated bridge fundamental period T_{SIB}(s)	2.19		
Effective yield strength of lead-core (MPa)	10.3		
Yield displacement of elastomeric bearing (mm)	7		
Shear modulus of rubber (MPa)	0.5		
$k_{d\text{-initial}}/k_u$ (Post-stiffness/ initial stiffness)	0.042	0.046	0.05
Lead core diameter D_{in}(mm)	70	100	100
External diameter D_{out}(mm)	410	520	540
Rubber layer thickness t_r(mm)	8	8	8
Thickness of an internal shim t_s(mm)	4	4	4
Number of layers (n)	34	24	24
Effective height H_{eff} (mm)	404	284	284

Table 3. Description of the ground motions used in the analyses

Earthquake	Year	$V_{s,30}$ (m/s)	Magnitude (M_w)	Station Name	R_{jb} (km)	PGA (g)
Northridge-01 (JGB)	1994	525.79	6.69	Jensen Filter Plant Generator Building	0.0	0.995
Loma Prieta	1989	380.89	6.93	Saratoga-Aloha Ave	7.58	0.514
Bam (Iran)	2003	487.4	6.6	Bam	0.05	0.808

Han *et al.* (2013) computed the ability of two analytical models for determining critical buckling loads and displacement in laterally deformed elastic bearings. It was found that increasing lateral displacement decreased the critical buckling load (P_{cr}) [26]. In the more conservative area-reduction method, the critical buckling load relies on lateral displacement [27]. That method calculates a zero capacity for a bearing at a lateral displacement equal to its own diameter, although experiments show that, even if the overlapping area reaches zero, the bearing will retain a minimum capacity [28-30]. Eq. (2) represents the bilinear model for calculating reduced buckling load capacity in bearing as suggested by Warn *et al.* (2007) [28]:

$$P'_{cr} = \begin{cases} \dfrac{A_r}{A} P_{cr} & \dfrac{A_r}{A} \ge 0.2 \\ 0.2 P_{cr} & \dfrac{A_r}{A} < 0.2 \end{cases} \qquad (2)$$

where P_{cr} and P'_{cr} are the critical buckling load of the LRB in the undeformed and deformed states, respectively, A_r is the reduced area of the elastomer bearing having diameter D due to lateral displacement u_h.

3.2.3 Coupled bi-directional motion

In order to study the coupling of bi-directional motion in the horizontal directions, the isotropic formulation of the model for restoring forces in orthogonal directions F_x and F_y was used [2, 31, 32].

4. STRONG GROUND MOTION IN NEAR-FAULT

Table 3 lists the characteristics of the three near-field earthquake records selected, including, magnitude, closest distance to fault plane (R_{rup}), peak ground acceleration and shear wave velocity of the top 30 m of the subsurface profile (V_{S30}). The selected accelerograms are compatible with soil type II. The selected acceleration records are scaled according to the seismic hazard level of the bridge site.

5. RESULTS AND DISCUSSION

Nonlinear time history analysis was applied to the seismically isolated bridge with LR isolators using OpenSees. Damping of the seismically isolated bridge (bridge structure with LR isolators) was assumed to be about 20% compatible with Rayleigh damping [33]. To evaluate the LRB responses, one central isolator that had been placed on the bridge pier or abutment was selected. All responses are provided for abutment 1 (A1), shortest pier (P1 & P7) and tallest pier (P4) (Fig.3).

5.1 Effect of normal force and buckling load capacity on LRB response

Fig.5(a) is an evaluation of the effect of normal force P on the response of LRB and the shear stiffness of the LRB as a function of P according to Eq. (1). Fig.5(b) shows the variation in shear stiffness of the LR isolator as a function of buckling load capacity (P'_{cr}) according to Eq. (1). As shown, the shear stiffness of the LRB decreased with an increase in

(a)   (b)
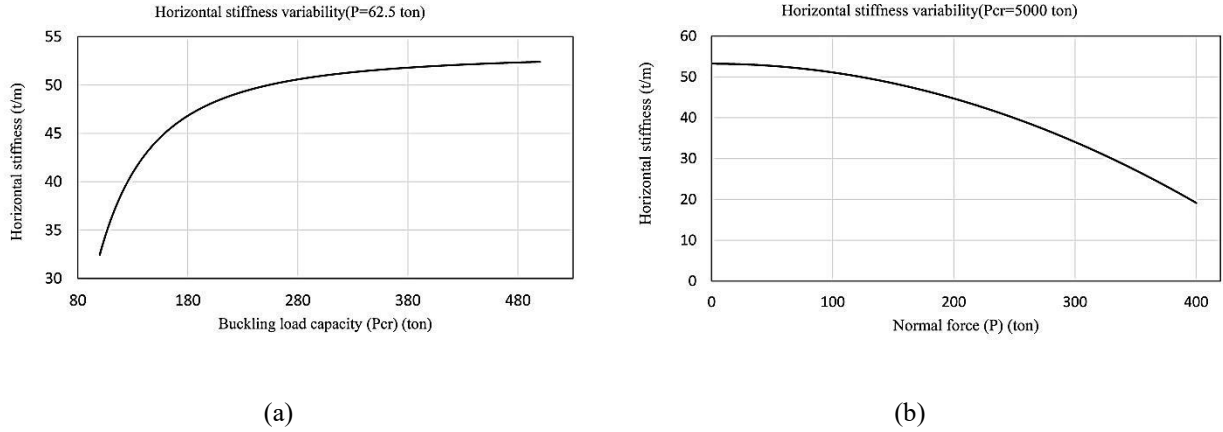
Fig. 5. Shear stiffness variability of the LR isolator as a function of the (a) applied normal force (P) and (b) buckling load capacity changes $(\mathbf{P}'_{\mathbf{cr}})$
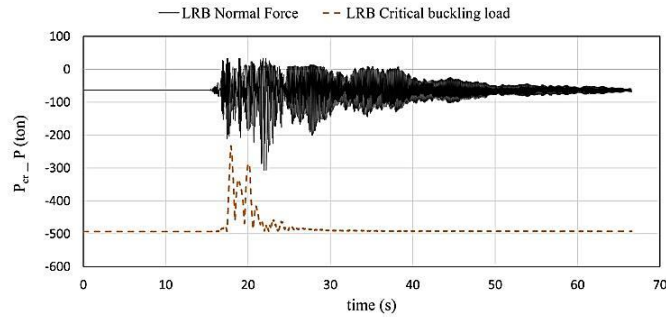
(a) Bam -Iran (2003) earthquake
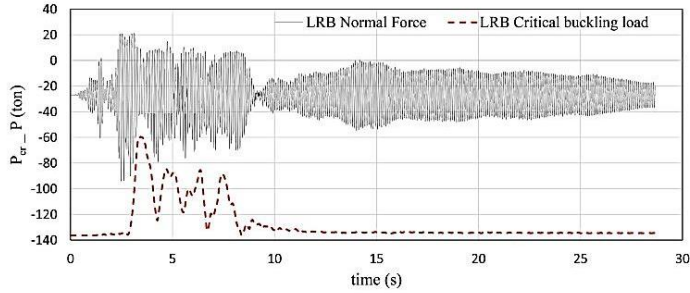
(b) Northridge-01 (JGB) (1994) earthquake

Fig. 6. Time history of axial load (P) versus the time history of critical buckling load capacity of LRB isolators.

P and a decrease in P'_{cr} as a parabola. The decrease in the shear stiffness of the LRB becomes essential only when the axial load approaches the critical buckling load capacity of the LRB. Fig.6 shows the axial load versus the critical buckling load capacity of the LRB over time.

The regions denoted by arrows in Fig.6 indicate that large horizontal displacement accompanied by a sudden increase in the compressive axial forces will create an important condition for the LRB isolators in which they will lose their resistance in some time instances during earthquake ground

motion. A decrease in the critical buckling load capacity of the LRB results from the imposed lateral displacement together with the increase in axial loading of the LRB due to the imposed vertical component. Eq. (1) indicates that $\left(P/P'_{cr}\right)^2$ increases in the form of a parabola and leads to a decrease in the shear stiffness (K_H) of the LRB (Fig.5). The decrease in shear stiffness also increases the horizontal displacement (u_h), thus reducing the vertical stiffness (K_v) and increasing the axial displacement of the LR isolators. This behavior is known as softening caused by the axial load under compression and is visible in the horizontal and vertical force-deformation

(a) Northridge-01 (JGB) (1994) earthquake   (b) Bam-Iran (2003) earthquake
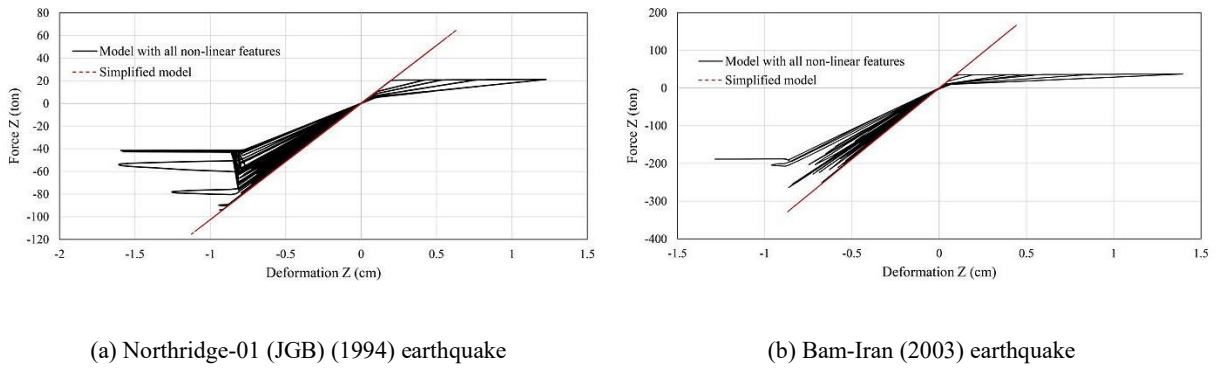
Fig. 7. Axial force-deformation curves including and excluding consideration of the main aspects of LRB modeling
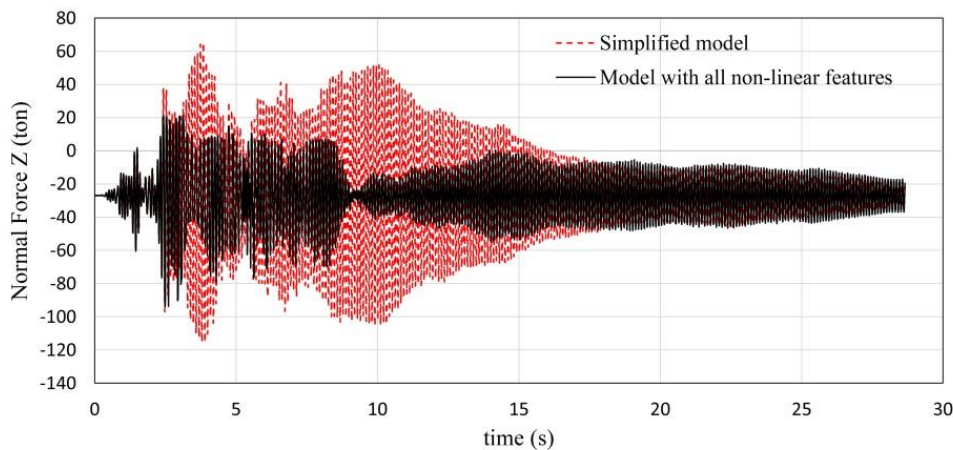
Fig. 8. Normal force time history of LR isolator including and excluding consideration of the main aspects of LRB modeling under the Northridge-01 (JGB) (1994) earthquake.
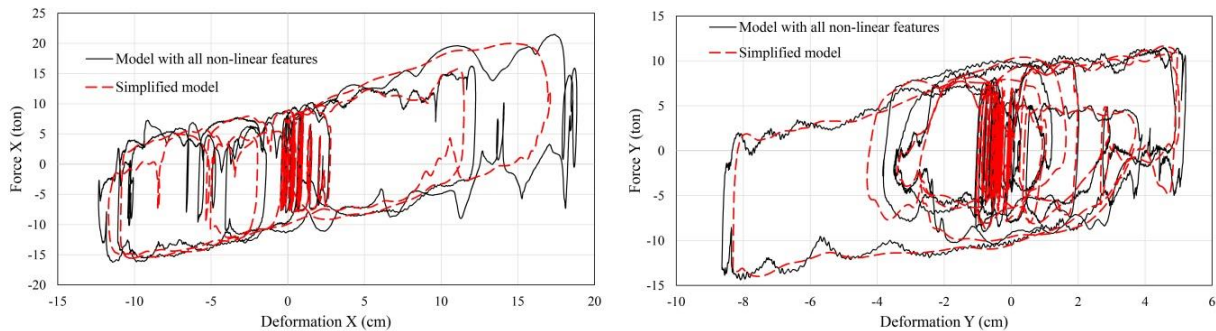
Fig. 9. Shear force-deformation curves in X and Y directions including and excluding consideration of the main aspects of LRB modeling for the Northridge (1994) earthquake.

curves of the LR isolators presented in the next sections.

This phenomenon is repeated at intervals during earthquake excitation and can lead to the complete loss of vertical resistance of the elastomeric bearing and cause buckling instability. This event is more likely in seismically isolated bridges with the elastomeric bearings under earthquakes with strong pulses in the ground velocity and displacement time histories of near-fault strong motion. The results show that the LR isolators on the bridge abutments (type 1) experienced a more critical situation than the other isolators. Because of this LRB behavior, the effect of

considering the main aspects of the LR on the seismically isolated bridge responses was studied.

5.1.1 Axial force versus deformation of LRB

Fig.7 shows the axial force-deformation curves for models that include and exclude the main aspects of elastomeric bearing. Fig.7 considers these main aspects in the LRB model and shows the cavitation starting point, post-cavitation behavior and strength degradation under cyclic loading in the tensile range of the axial force-deformation curves of the LR isolator (as denoted by arrows). In the compressive
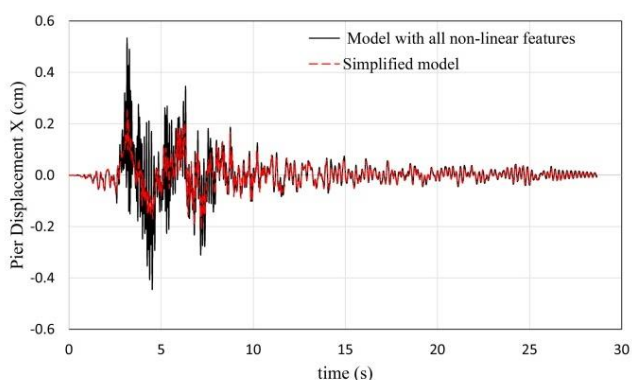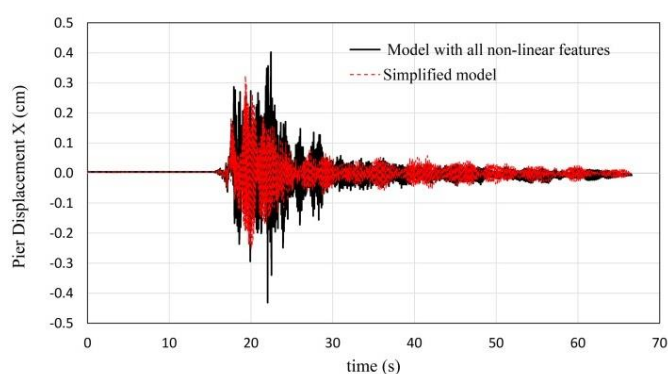
(a) Northridge-01 (JGB) (1994) earthquake (b) Bam Iran (2003) earthquake

Fig. 10. Displacement time history of bridge piers including and excluding consideration of the main aspects of LRB modeling.
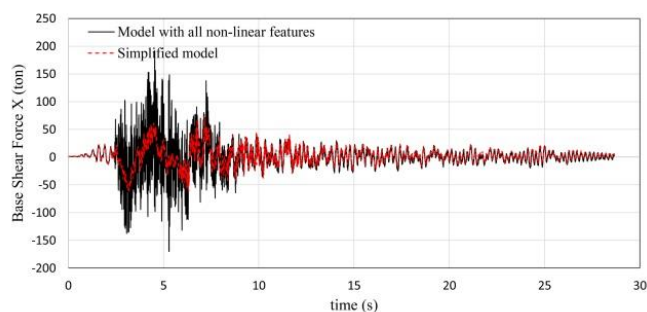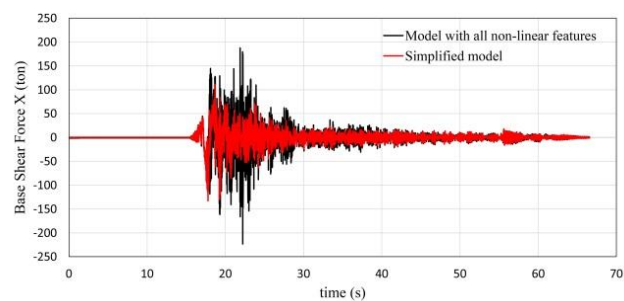
(a) Northridge-01 (JGB) (1994) earthquake (b) Bam Iran (2003) earthquake

Fig. 11. Base shear force time history of bridge columns including and excluding consideration of the main aspects of LRB modeling.

range of the axial force-deformation curves of the LR isolator, force softening under compression due to increased lateral displacement as well as a sharp decrease in vertical resistance caused by the large lateral displacement is shown. When excluding the main aspects in the modeling of LRB, none of these behaviors can be observed and axial force-deformation appears to be perfectly linear. Fig.8 shows the normal force time history of the LR isolator for the two models. As seen, lack of consideration of the cavitation behavior in tension and force softening under compression produces a large axial force and small axial displacement.

5.1.2 Shear force versus deformation of LR isolators

The shear force-deformation curves of the LR isolators when the main aspects of elastomeric bearing are considered shows considerable distortion in the post-elastic stiffness (Fig.9). This post-elastic stiffness is a direct function of the normal force variation imposed by the vertical component of strong ground motion. When these main aspects of the LRB are not considered, the post-elastic stiffness appears to be more smooth and uniform in the shear force-deformation curves of the LR isolators. This phenomenon results from

disregarding the normal force (P) and buckling load capacity (P'_{cr}) and changes in the shear post-elastic stiffness.

5.1.3 Displacement time history of bridge piers

Fig.10 shows the effect of including the main aspects of the LRB on the displacement time history of the bridge piers. When the shear post-elastic stiffness deviation is disregarded, the buckling load capacity and axial load applied to the LR isolator become constant during earthquake excitation and are considered equal to the initial nominal capacity of the critical buckling load in the laterally non-deformed state and gravity load, respectively. This assumption leads to constant shear post-elastic stiffness of the LR isolators during the earthquake excitation. On the other hand, vertical excitation in some time instances reduces the axial load applied to the LR isolator relative to the applied initial gravity load. At some time intervals of earthquake excitation, the LR isolator is located under the tensile axial load. This event increases post-elastic shear stiffness (Fig.5) as well as increasing the displacement demand on the bridge piers. It can be seen that exclusion of the main aspects of the LRB causes a smaller displacement value for the bridge piers compared to actual conditions.

284
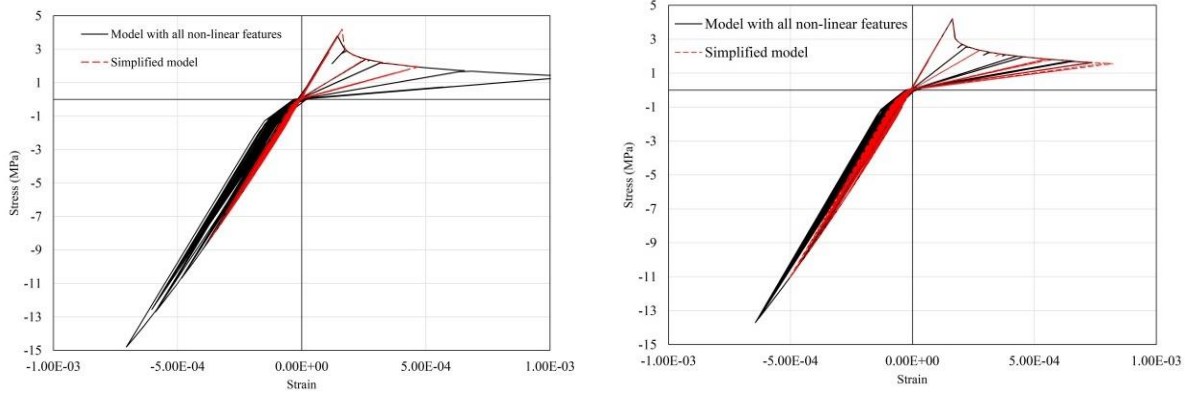
(a) Northridge-01 (JGB) (1994) earthquake

(b) Bam Iran (2003) earthquake

Fig. 12. Stress-strain curves of column base including and excluding consideration of the main aspects of elastomeric bearing modeling.

Table 4. Average variation rate (in percent) of maximum values of base shear force of bridge pier columns

Title	Column 1 of pier		Column 2 of pier	
Direction	Longitudinal	Transverse	Longitudinal	Transverse
Pier 1	56.8	-19.84	48.86	-17.7
Pier 2	36.0	29.8	30.48	21.01
Pier 3	85.1	12.64	62.58	1.87
Pier 4	36.7	14.47	37.47	5.12
Pier 5	82.9	-3.5	81.33	-0.78
Pier 6	74.7	1.0	72.48	9.41
Pier 7	116.2	-0.3	108.38	-3.2

Table 5. Average variation in ratio of maximum displacement of bridge piers and deck

Title	Bridge deck (%)		Bridge pier (%)	
Direction	Longitudinal	Transverse	Longitudinal	Transverse
Abut 1	7.2	2.96	------	------
Pier 1	7.2	2.96	20.43	-36.68
Pier 2	7.2	3.1	59.3	31.2
Pier 3	7.2	3.2	86.25	-5.88
Pier 4	7.2	3.2	60.76	4.46
Pier 5	7.2	3.16	112.8	-5.76
Pier 6	7.2	3.3	61.03	-19.9
Pier 7	7.2	3.63	81.5	-29.42
Abut 2	7.2	3.8	------	------

5.1.4 Base shear force time history of bridge columns

The base shear force of the bridge columns is displayed in Fig.11 for both models. An increase in deformation demand of the bridge piers increased the base shear force of the bridge columns. It can be seen that disregarding the main aspects of the LRB modeling produced a smaller base shear force for the bridge columns.

5.1.5 Column base stress-strain curve

When the main aspects of the LRB model were considered, the column bases experienced larger stress-strain values and some column bases were on the verge of forming

a plastic hinge. As seen in Fig.12(a), when considering the main aspects of LRBs, the column base for column 1 in the tallest pier $(P4)$ experienced stress of about 15 MPa under the Northridge-01 (JGB) earthquake records. When the main aspects were ignored, the stress decreased to 8 MPa. Failure to consider the main aspects of the LRB did not allow conservative assessment and design of a seismically isolated bridge. Accordingly, because AASHTO regulations require a seismically isolated bridge substructure to remain in the linear range, the nonlinear behavior will be ignored for some piers of a seismically isolated bridge under near-fault strong ground motion.

5.2 Numerical results and discussion

The seismically isolated bridge responses were calculated using the following relationship including and excluding the main specifications of LRB behavior:

$$\left(\left(R_{max.with} - R_{max.without} \right) / R_{max.without} \right) *100$$

where $R_{max.with}$ is the maximum response considering the main aspects of LRB and $R_{max.without}$ is the maximum response of the seismically isolated bridge using the simplified behavioral model for LRBs. Tables 4 and 5 show the average increase (+) or decrease (-) in the maximum value of the base shear force of bridge abutments and columns and the displacement of bridge piers and displacement of the bridge deck, respectively.

After applying the main aspects of the nonlinear behavior of the LRBs, the average maximum base shear force increased about 116% in the longitudinal direction and about 29.8% in the transverse direction in comparison with a simple modeling. It also increased the average maximum displacement of bridge pier about 113% in the longitudinal direction and 31% in the transverse direction. Consideration of the main aspects increased the average maximum displacement of the bridge deck about 7.2% in the longitudinal direction and 3%-4% in the transverse direction.

6. CONCLUSIONS

The present study modeled seismically isolated bridges with LRBs in OpenSees software. The responses of the isolated bridge while including or excluding the main aspects of LRB behavior in modeling were compared under strong near-fault ground motion. The following results were obtained:
· The shear stiffness of the LRB decreases as the axial load P increases and decreases the buckling load capacity P'_{cr} as a parabola. A decrease in the shear stiffness of the LRBs becomes important only when the axial load approaches the critical buckling load capacity of the LRBs.
· The simultaneity of large horizontal displacement and the sudden increase in the compressive axial forces causes the LRBs to experience a critical condition in some earthquakes and significantly lose their resistance.
· Excluding the cavitation behavior under tension and force softening under compression produces a larger axial force and smaller axial displacement than when including the main aspects of the LRB.

· Ignoring the main aspects of LRBs leads to smaller estimated displacement of the bridge piers than that is found in actual conditions.
· The results revealed that the average maximum base shear force in the bridge piers increased about 116% and 29.8% in the longitudinal and transverse direction respectively in comparison with the simple modeling. It also increased the average maximum displacement of bridge pier about 113% in the longitudinal direction and 31% in the transverse direction
· Disregarding the main aspects of the LRBs produces smaller stress and base shear forces of the bridge columns relative to actual conditions. Because the AASHTO regulation requires a seismically isolated bridge substructure to remain in the linear range, with the simple model for LRBs, the nonlinear behavior of some columns of isolated bridges will be ignored under strong near-fault ground motion.

REFERENCES

[1] M. Saiidi, E. Maragakis, G. Griffin, Effect of base isolation on the seismic response of multi-column bridges, Structural Engineering and Mechanics, 8(4) (1999) 411-419.

[2] M. Kumar, A.S. Whittaker, M.C. Constantinou, An advanced numerical model of elastomeric seismic isolation bearings, Earthquake Engineering & Structural Dynamics, 43(13) (2014) 1955-1974.

[3] I. Buckle, S. Nagarajaiah, K. Ferrell, Stability of elastomeric isolation bearings: Experimental study, Journal of Structural Engineering, 128(1) (2002) 3-11.

[4] C.G. Koh, J.M. Kelly, Effects of axial load on elastomeric isolation bearings, (1987).

[5] M. Kumar, A.S. Whittaker, M.C. Constantinou, Experimental investigation of cavitation in elastomeric seismic isolation bearings, Engineering Structures, 101 (2015) 290-305.

[6] K. Ishii, M. Kikuchi, T. Nishimura, C.J. Black, Coupling behavior of shear deformation and end rotation of elastomeric seismic isolation bearings, Earthquake engineering & structural dynamics, 46(4) (2017) 677-694.

[7] K. Ishii, M. Kikuchi, Improved numerical analysis for ultimate behavior of elastomeric seismic isolation bearings, Earthquake Engineering & Structural Dynamics, 48(1) (2019) 65-77.

[8] C.-y. Shen, P. Tan, J. Cui, Y.-h. Ma, X.-y. Huang, Critical tension–shear load of elastomeric seismic isolators: An experimental perspective, Engineering Structures, 121 (2016) 42-51.

[9] Z. Zhang, X. Liu, Y. Peng, Improved nonlinear rotational constitutive law for predicting critical loads in elastomeric isolation bearings, Construction and Building Materials, 211 (2019) 150-158.

[10] A. Elgamal, L. He, Vertical earthquake ground motion records: an overview, Journal of Earthquake Engineering, 8(05) (2004) 663-697.

[11] W. Silva, Characteristics of vertical strong ground motions for applications to engineering design, 1088-3800, 1997.

[12] M. Eröz, R. DesRoches, A comparative assessment of sliding and elastomeric seismic isolation in a typical multi-span bridge, Journal of Earthquake Engineering, 17(5) (2013) 637-657.

[13] G.P. Warn, A.S. Whittaker, Vertical earthquake loads on seismic isolation systems in bridges, Journal of structural engineering, 134(11) (2008) 1696-1704.

[14] M.R. Button, C.J. Cronin, R.L. Mayes, Effect of vertical motions on seismic response of highway bridges, Journal of structural engineering, 128(12) (2002) 1551-1564.

[15] S. Chen, T. Wang, W. Yan, Z. Zhang, K.-S. Kim, Theoretical tensile model and cracking performance analysis of laminated rubber bearings under tensile loading, Structural Engineering and Mechanics, 52(1) (2014) 75-87.

[16] B. Olmos, J. Roesset, Effects of the nonlinear behavior of lead-rubber bearings on the seismic response of bridges, Earthquakes and Structures, 1(2) (2010) 215-230.

[17] A. Aviram, K.R. Mackie, B. Stojadinović, Guidelines for nonlinear analysis of bridge structures in California, Pacific Earthquake Engineering Research Center, 2008.

[18] S. Mazzoni, F. McKenna, M.H. Scott, G.L. Fenves, The open system for earthquake engineering simulation (OpenSEES) user command-language manual, (2006).

[19] K.L. Ryan, B. Richins, Design, Analysis, and Seismic Performance of a Hypothetical Seismically Isolated Bridge on Legacy Highway, Utah Department of Transportation, 2011.

[20] I. Buckle, M. Al-Ani, E. Monzon, Seismic isolation design examples of highway bridges, NCHRP Project, (2011) 20-27.

[21] G.P. Warn, A.S. Whittaker, A study of the coupled horizontal-vertical behavior of elastomeric and lead-rubber seismic isolation bearings, No. MCEER-06-0011. Multidisciplinary Center for Earthquake Engineering Research, 2006.

[22] AASHTO, Guide specifications for seismic isolation design, American Association of State Highway and Transportation Officials , 2010.

[23] V&V ASME , Guide for verification and validation in computational solid mechanics, American Society of Mechanical Engineers, 2006.

[24] G.P. Warn, The coupled horizontal-vertical response of elastomeric and lead-rubber seismic isolation bearings, State University of New York at Buffalo, 2006.

[25] J.M. Kelly, Earthquake-resistant design with rubber, (1993).

[26] X. Han, C.A. Kelleher, G.P. Warn, T. Wagener, Identification of the controlling mechanism for predicting critical loads in elastomeric bearings, Journal of Structural Engineering, 139(12) (2013) 04013016.

[27] I.G. Buckle, Stability of elastomeric seismic isolation systems, in: Proc. of Seminar on Seismic Isolation, Passive Energy Dissipation and Control, 1993, Applied Technology Council, 1993.

[28] G.P. Warn, A.S. Whittaker, M.C. Constantinou, Vertical stiffness of elastomeric and lead–rubber seismic isolation bearings, Journal of Structural Engineering, 133(9) (2007) 1227-1236.

[29] J. Weisman, G.P. Warn, Stability of elastomeric and lead-rubber seismic isolation bearings, Journal of Structural Engineering, 138(2) (2011) 215-223.

[30] J. Sanchez, A. Masroor, G. Mosqueda, K. Ryan, Static and dynamic stability of elastomeric bearings for seismic protection of structures, Journal of structural engineering, 139(7) (2012) 1149-1159.

[31] M. Constantinou, A. Mokha, A. Reinhorn, Teflon bearings in base isolation II: Modeling, Journal of Structural Engineering, 116(2) (1990) 455-474.

[32] A. Mokha, M. Constantinou, A. Reinhorn, Teflon bearings in base isolation I: Testing, Journal of Structural Engineering, 116(2) (1990) 438-454.

[33] H. Ounis, A. Ounis, Effect Of The Damping Of The LRB System On The Dynamic Response Of A Base Isolated Building, in: Turkish Conference on Earthquake Engineering and Seismology–TDMSK, Antakya, Hatay/ Turkey, 2013.